Adsorption of congo red onto activated carbons having different surface properties: studies of kinetics and adsorption equilibrium

Meriem Belhachemi[a,b,*], Fatima Addoun[b]

[a]Laboratoire de Fiabilité des matériaux et des structures en région sahariennes, Faculté des Sciences et Technologie, Université de Béchar, B.P. 417, Béchar 08000, Algeria
Tel. +21349815591; Fax: +21349815244; email: bel_meriem@yahoo.fr
[b]Laboratoire d'étude physico-chimique des matériaux et application à l'environnement, Faculté de Chimie, USTHB, B.P. 32, El Alia 16111 Bab Ezzouar Alger, Algeria

ABSTRACT

To enhance congo red (CR) removal from aqueous solution, activated carbons prepared from date pits and modified by oxidation with nitric acid followed by heat treatment in a nitrogen atmosphere were tested. Kinetic and equilibrium adsorptions data of CR from aqueous solution were carried out, showing that the elimination of oxygen surface groups from activated carbon by heat treatment enhanced the adsorption capacity. The adsorption followed pseudo-second order kinetics. The experimental isotherms were analysed with two and three parameters equations (Freundlich, Langmuir, and Redlich–Peterson) using non-linear regression. The results showed that the Langmuir and Redlich–Peterson isotherms best-fit the equilibrium data, with maximum adsorption capacity of 105 mg/g calculated from Langmuir equation. The mechanism adsorption of this anionic dye on activated carbons involved electrostatic and dispersive interactions.

Keywords: Activated carbon; Surface properties; Dye; Adsorption; Kinetics; Isotherms

1. Introduction

Activated carbons are the most popular adsorbents used for the removal of toxic substances from water. This could be related to their extended surface area, high adsorption capacity, microporous structure and special surface reactivity [1]. However, the adsorptive capacity of activated carbons depends mainly on the precursor nature, the operating conditions of adsorption and the nature of the adsorbate. The carbon precursors may be of botanical origin (wood, coconut shells, fruit seeds), mineral origin (coal, peat), or polymeric materials (rubber tyres, plastics). About 50% of industrially available activated carbons are derived from precursors of lignocellulosic origin [2,3].

Date pits are among the most common agricultural by-products available commercially in the palm growing countries such as Algeria. Pits of date palm are a waste product of many industries, after technological transformation of the date fruits. Date stones constitute roughly 10% in weight of the fruit [4]. Therefore, any attempt to reuse this waste will be useful for these countries.

Several industries, such as textile, ceramic, paper, printing and plastic use dyes in order to colour their products. In the colouring process, these industries also consume substantial volumes of water, and as a result, large amount of coloured wastewater are generated. The presence of dyes in water is undesirable since even a very small amount of these colouring agents is highly visible and may be toxic to aquatic environment [5]. The treatment of contaminated congo red in wastewater is not straightforward, since the dye is generally present in
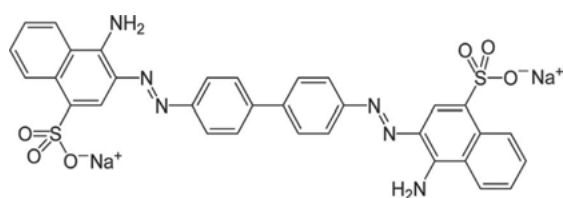
_____

*Corresponding author.

Fig. 1. Molecular structure of congo red.

sodium salt form giving it a very good water solubility. Also, the high stability of its structure makes it difficult to biodegrade and photodegrade. Several methods are available for colour removal from wastewater such as: membrane separation, aerobic and anaerobic degradation using various micro organisms, chemical oxidation, coagulation and flocculation, adsorption using different kinds of adsorbents and reverse osmosis. Among them, adsorption is a promising removal technique that produces effluents containing very low levels of dissolved organic compounds.

In this work, the activated carbon prepared from date pits by thermal activation, and modified by selected oxidation and heat treatments were tested to remove congo red dye (Fig. 1 molecular structure). Our goal is to study the interactions between activated carbon surface, and the anionic dye in order to develop optimised adsorbent materials for the decolourization of wastewaters.

2. Experimental methods

2.1. Preparation of activated carbons

The starting activated carbon used in this work is an activated carbon prepared from date pits by thermal activation with CO_2. This material was submitted to two different modifications, oxidation with HNO_3 and thermal treatment with N_2, in order to produce samples with different surface properties. The samples are labeled as follows: C37 (parent activated carbon issued from date pits); C37N (sample C37 oxidized in the liquid phase with HNO_3 14M at boiling temperature during 10 min); C37NT (sample C37N thermally treated under N_2 flow at 700°C for 1 h. Further experimental details can be found in reference [6].

2.2. Characterization of activated carbons

The textural and surface chemical properties of the activated samples were obtained by the following techniques:

N_2 and CO_2 adsorption–desorption isotherms were obtained in a static manometric apparatus at –196°C and 0°C, respectively. The specific surface area (S_{BET}) was

obtained using the BET method. The micropore volume, V_{N_2} and the volume of narrow micropores, V_{CO_2} were obtained by application of the Dubinin–Raduskevich equation to the adsorption isotherm of N_2 and CO_2, respectively. Finally, the mesopore volume (V_{meso}) was estimated by subtracting the micropore volume (V_{N_2}) from the total volume adsorbed at $P/P_o = 0.95$.

Temperature-programmed desorption experiments under helium were carried out to evaluate the amount and nature of the oxygen surface groups present in each sample. Thus, 100 mg of sample were placed in a U-shape quartz reactor on-line coupled to a quadrupole mass spectrometer (Balzer MSC200). The experiments were performed up to 1000°C under a He flow (50 ml/min) and a heating rate of 10 K/min. The amount of CO and CO_2 evolved were quantified after calibration with a calcium oxalate ($CaC_2O_4 \cdot H_2O$) standard. In addition, Fourier Transform infra-red spectroscopy (FTIR) was used to characterize the oxygen surface groups. The FTIR spectra of the samples were obtained by using KBr wafers containing 0.5 g of carbon.

The pH_{PZC}, i.e., pH of the point zero charge was measured. For this purpose, 50 ml of a 0.01M NaCl solution was placed in a 100 ml Erlenmeyer flask. Then, the pH was adjusted to successive initial values between 2 and 12, by using either NaOH or HCl, and 0.15 g of AC was added to the solution. After a contact time of 48 h, the final pH was measured and plotted against the initial pH. The pH at which the curve crosses the line pH (final) = pH (initial) is taken as the pH_{PZC} of the activated carbon considered.

2.3. Adsorption experiments

The equilibrium adsorption isotherms at 25°C were obtained by introducing 10 ml of dye solutions of different concentrations with 10 mg of the activated carbons into well-closed flasks. Then, all the flasks were shaken for 24 h. It was tested by kinetic experiments that this period of time was enough to reach equilibrium adsorption for all adsorbents. After shaking, the suspension was centrifuged, and the concentration was measured with a Unicam helios δ UV–visible spectrophotometer at 497 nm, which was the maximum wave length for CR. Dilution was undertaken when absorbance exceeded 1.0. The final concentration of the solution was then determined from the calibration curve. In these sorption experiments, the solution pH was used without adjustment. The pH of all solutions in contact with adsorbent was found to be in the range 5.5–6.5.

The amount of CR adsorbed was calculated by

$$q_e = \frac{(C_0 - C_e)}{m} V \tag{1}$$

where q_e is the amount of dye adsorbed in activated carbon, C_o and C_e are the initial and equilibrium concentrations of adsorbates solutions, m is the amount of adsorbent and V is the volume of solution.

The effect of contact time on the amount of dye adsorbed was investigated at the optimum initial concentration of dye. The initial concentration was 100 mg/l.

3. Results and discussion

3.1. Activated carbon characterization

Table 1 reports the texture parameters obtained from N_2 and CO_2 adsorption at –196°C and 0°C, respectively. The results show that the oxidation treatment of sample C37 with (HNO_3) produces some changes in the adsorption properties. The oxidized sample (C37N) exhibits a decrease in the surface area and in the total pore volume, with mainly no change in the narrow micropore. The newly created oxygen surface groups located in the pore mouth of the micropores gives rise to diffusional restrictions for the N_2 molecule at –196°C. However, a subsequent heat treatment at 700°C with N_2 causes the removal of an important part of the oxygen surface groups (the less stable groups, evolved as CO_2 in temperature-programmed experiments, together with part of the more stable and less acidic oxygen groups, which evolve as CO), and their corresponding carbon atoms (selective gasification) giving rise to an increase in the surface area and pore volume (Table 1).

The relative thermal stability of surface functional groups is often used as a measurement of the concentration of these functionalities on the carbon surface. The temperature-programmed desorption experiments gives the amount and the nature of oxygen surface groups. During a TPD experiment, surface oxygen groups on carbon materials are decomposed upon heating by releasing CO_2 at lower temperatures and predominantly CO at higher temperatures. Treatments with HNO_3 originate materials with large amounts of surface acidic groups, mainly carboxylic acids and, in less extent lactones, anhydrides and phenol groups [7].

The oxidation treatment with HNO_3 (14 M) of C37 carbon, produces important changes in the surface chemistry. As it can be observed in Table 2, the oxidized sample (C37N) exhibits an important increase in the total amount of oxygen surface groups evolved both as CO_2 and CO, this enhancement being higher for the CO_2 groups (lower CO/CO_2 ratio). The subsequent thermal treatment at temperature (700°C) produces the suppression of the less stable groups (evolved as CO_2) together with an important decrease in the amount of CO, which is clearly reflected by the increase in the CO/CO_2 ratio. The sample retains the most stable oxygen groups, which can be assigned to basic groups. Similar results have been reported in the literature [7,8].

The FTIR spectrum of the activated carbons (C37, C37N and C37NT) are shown in Fig. 2. The samples show absorption at approximately 3437 and 3463 O-H) that can be assigned to carboxylic acid groups and 2923 C-H) present in quinone. After oxidation, new bands appeared at 1585 cm^{-1} and 1383 cm^{-1} in C37N which are characteristic of C–O and C=O, these indicate the presence of ethers, lactones and nitro groups [8,9]. For C37NT, the intensity of characteristic –OH band of

Table 2
Amount of CO_2 and CO evolved during TPD experiments of the activated carbon samples

Activated carbons	CO_2 (mmol/g)	CO (mmol/g)	CO/CO_2	pH_{PZC}
C37	0.43	1.17	2.72	8.2
C37N	1.04	2.55	2.45	3.2
C37NT	0.15	0.92	6.13	8.8

Table 1
Surface area, micropore volume and mesopore volume of activated carbon samples

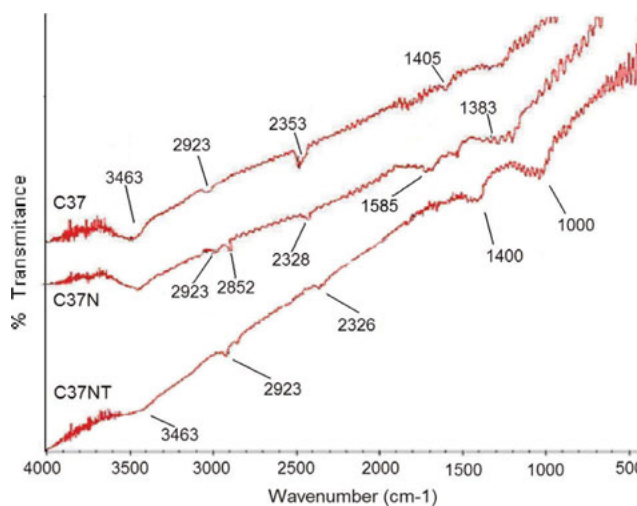| Sample	S_{BET} (m²/g⁻¹)	V_{N_2} (cm³/g⁻¹)	V_{meso} (cm³/g⁻¹)	V_{TN_2} (cm³/g⁻¹)	V_{CO_2} (cm³/g⁻¹)
C37	1069	0.44	0.08	0.52	0.36
C37N	950	0.37	0.05	0.42	0.35
C37NT	1160	0.46	0.07	0.53	0.39

Fig. 2. FTIR spectra of C37, C37N and C37NT activated carbons.

carboxylic acid groups disappeared, because heat treatment induces decomposition of acidic groups. This result has been proved by TPD experiments.

The point of zero charge describes the condition when the electrical charge density on a surface is zero. The pH of point of zero charge (pH_{PZC}) of an activated carbon depends on the chemical and electronic properties of the functional groups on its surface and is a good indicator of these properties. The measured pH_{PZC} values of C37, C37N and C37NT are 8.2, 3.2 and 8.8 respectively. Generally, the surface of activated carbon is positively charged at $pH < pH_{PZC}$ and negatively charged at $pH > pH_{PZC}$. The different pH_{PZC} values of the three AC samples reveal that over a particular pH range, different ionic species will be formed, generating different charges on the carbon surface. Negative surface charge is produced by dissociation of surface oxygen complexes of acidic character, e.g., carboxylic acid and phenolic groups. The data in Table 2 show that for an aqueous solution of CR that has not been pH adjusted, the carbon surface will be negatively charged for C37N and positively charged for C37 and C37NT.

Finally, the results obtained from the different techniques, show that sample C37N has a strong acid character while C37 and C37NT have basic characteristics.

3.2. Adsorption kinetics

Fig. 3 illustrates the kinetics of dye removal for the three activated carbons at 25°C. The effect of contact time on the amount of CR adsorbed has been investigated at the optimum initial concentration of dye. Fig. 3 shows that the removal of CR by these activated carbons increases and reaches a maximum value with the increase in contact time. C37NT shows the highest CR adsorption performance.

In order to investigate the adsorption kinetics of CR, three kinetic models, namely pseudo-first-order, pseudo-second-order and intraparticle diffusion models, were used in this study.

The pseudo-first-order Lagergren equation is given by

$$\frac{dq_t}{dt} = k_1(q_e - q_t) \tag{2}$$

where k_1 is the rate constant for the first order (min⁻¹). Integrating Eq. (2) for the boundary conditions $t = 0 - t$ and $q_t = 0 - q_t$ gives

$$q_t = q_e(1 - \exp(-k_1 t)) \tag{3}$$

Eq. (3) may be written in linear form:

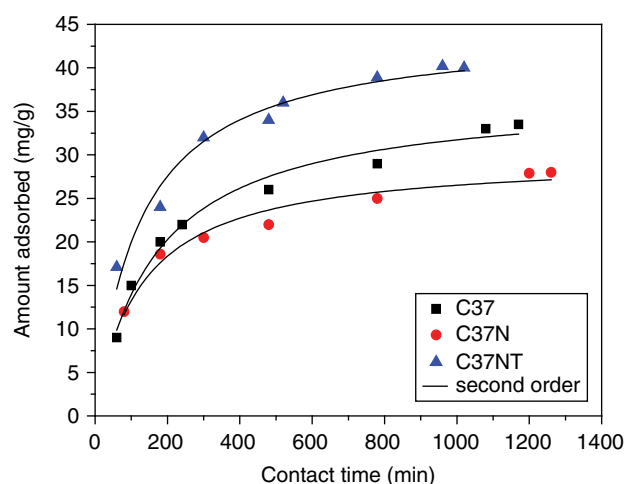Fig. 3. Kinetic curves for the adsorption of CR on activated carbons at 25°C.

$$\log(q_e - q_t) = \log q_e - \frac{k_1 t}{2.303} \tag{4}$$

The first order kinetics constants for the adsorption of CR on three activated carbons obtained from the slope and the intercept of the linear plots of versus t are given in Table 3. The correlation coefficients values obtained are between 0.92 and 0.98. Furthermore, the calculated values q_e are not in agreement with the experimental values $q_{e,exp}$, showing that the adsorption kinetics did not follow the pseudo-first-order model.

In the last years, the pseudo-second-order kinetic model has been considered to be the most appropriate and widely used to describe the adsorption kinetics. The pseudo-second-order equation is expressed as

$$q_t = \frac{k_2 q_e^2 \, t}{1 + k_2 q_e t} \tag{5}$$

where k_2 (g/mg min) is the rate constant. Eq. (5) can be linearized to:

$$\frac{t}{q_t} = \frac{1}{k_2 q_e^2} + \frac{1}{q_e} t \tag{6}$$

The values of k_2 were calculated from the slopes of the respective linear plots of $\frac{t}{q_t}$ versus t (Fig. 4a).

The initial adsorption rate, h (mg/g min) at $t \to 0$ is defined as

$$h = k_2 q_e^2 \tag{7}$$

Table 3
Kinetic parameters of the pseudo-first-order, pseudo-second-order and intraparticle diffusion models for congo red adsorption

Activated carbon	1st order model				2nd order model				Intraparticle model	
	q_{exp} (mg/g)	q_e (mg/g)	k_1 (min^{-1})	R^2	q_e (mg/g)	h (mg/g min)	k_2 (g/mg min)	R^2	k_p (mg/g min$^{1/2}$)	R^2
C37	33.5	24.5	2.3×10^{-3}	0.92	36.0	0.27	2.1×10^{-4}	0.99	0.81	0.92
C37N	28.0	15.7	2.1×10^{-3}	0.98	33.2	0.14	1.2×10^{-4}	0.98	0.53	0.92
C37NT	40.2	30.9	3.9×10^{-3}	0.97	45.2	0.34	1.6×10^{-4}	0.99	1.00	0.93

Kinetic constants and correlation coefficients, R^2 of the pseudo-second order model for activated carbons are listed in Table 3. Figs. (3, 4a) depict the applicability of this model on the kinetics adsorption of CR on activated carbons. As it can be observed correlation coefficients are equal to 0.99 for almost all systems (Table 3). Also, the $q_{e,exp}$ and q_e values from pseudo second order

Fig. 4. Kinetics for adsorption of CR onto activated carbons: (a) pseudo-second order; (b) intraparticle diffusion model.

kinetic model are relatively similar to each other, indicating that the Congo red adsorption obeys the pseudo-second-order kinetic model. Considering the initial adsorption rate (h), the results reveal that C37NT (basic carbon) was faster than that of C37N (acidic carbon). It is worth nothing that C37NT (heat treated carbon) may perform better removal efficiency. Similar kinetic results have also been reported for the adsorption of Direct Yellow 12 onto activated carbons and methylene blue onto date pits and palm trees [10,11].

The intra-particle-diffusion equation is expressed as

$$q_t = k_p t^{1/2} \tag{8}$$

where k_p (mg/g min$^{1/2}$) is the intraparticle diffusion rate constant. According to Eq. (8) a plot of q_t versus $t^{1/2}$ should be a straight line with a slope k_p when adsorption mechanism follows the intra-particle diffusion process. Fig. 4b, presents a plot of q_t versus $t^{1/2}$ for all the three activated carbons. As it can be observed, there are two different regions. The initial portion was the surface adsorption or rapid external diffusion stage. The second linear portion is the gradual adsorption stage controlled by intraparticle diffusion. The values of k_p as obtained from the plots are listed in Table 3. This finding is in good agreement with many others reports published on reactive orange and malachite green dyes adsorption [12,13].

3.3. Adsorption isotherms

Fig. 5 shows the adsorption isotherms of CR on the three activated carbons at 25° C. The three activated carbons presented L type according to the Giles classification. The equilibrium adsorption capacity of these samples increased with increasing dye concentration and reached a maximum at about a concentration of 400 mg/g. The plateau in adsorption revealed that CR was adsorbed as a monolayer on activated carbons. Three adsorption isotherm models were used in this work, Langmuir, Freundlich and Redlich–Peterson Isotherms.
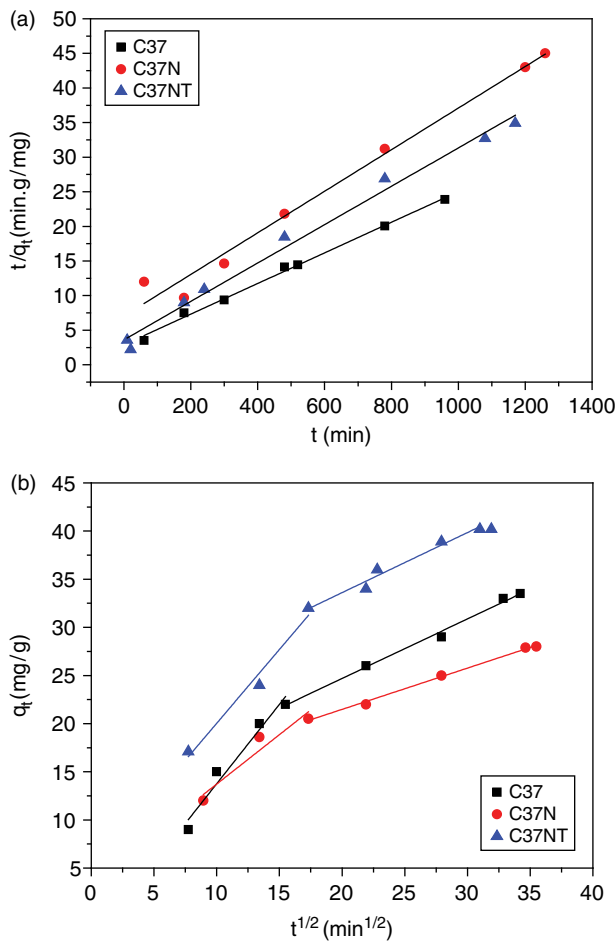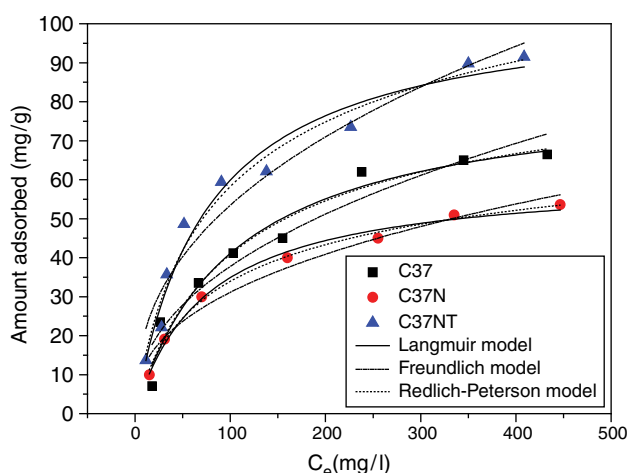
Fig. 5. Adsorption equilibrium isotherms of CR on activated carbons at 25°C.

The Freundlich isotherm is an empirical equation that is also often used to correlate adsorption experimental data. The Freundlich isotherm equation has the following form

$$q_e = k_F \cdot C_e^{1/n} \qquad (9)$$

where k_F is the Freundlich constant related to the adsorption capacity $(mg/g)(mg/l)^n$ and parameter n characterize the heterogeneity of the system.

Langmuir model is the most widely used isotherm equation, which has the form as follows

$$q_e = \frac{Q_0 K_L C_e}{1 + K_L C_e} \qquad (10)$$

where Q_0 and K_L are Langmuir isotherm parameters, representing the maximum uptake capacity per unit mass of carbon (mg/g), and the Langmuir constant (l/mg) respectively.

The Redlich–Peterson (R-P) isotherm model can be represented by Eq. (11):

$$q_e = \frac{K_R C_e}{1 + a_R C_e^{\beta}} \qquad (11)$$

where K_R is the R-P isotherm constant (l/mg), a_R is also a constant $(l/mg)^{1/\beta}$ and β is the exponent which lies between 0 and 1.

The R-P isotherm has a linear dependence on concentration in the numerator and an exponential function in the denominator. It approaches the Freundlich model at high concentrations and is in accord with the low concentration limit of the Langmuir equation. Furthermore, the R-P equation incorporates three parameters into an empirical isotherm, and therefore, can be applied either in homogenous or heterogenous systems due to its high versatility.

Fig. 5 shows that Langmuir and R-P isotherms can describe the experimental fairly well. Table 4 summarizes all the constants obtained for the three isotherm models using non linear regression, Origin software was used for fitting data. The comparisons of linear and nonlinear regressions often concluded that the best parameter estimates were returned by nonlinear optimizations [14,15]. The correlation coefficients for Freundlich isotherm are significantly less than that of Langmuir and Redlich–Peterson isotherms. The Langmuir and R-P adsorption isotherms yield the best fit, as the R^2 values are relatively high and similar. From Freundlich isotherm model, the $1/n$ values obtained for all activated carbons are below one. This indicates that the adsorption process followed a normal Langmuir isotherm [16]. In relation to the R-P equation, it can be seen that for the constant $\beta = 1$, Eq. (10) reduces to Langmuir equation and for $\beta = 0$, it reduces to Henry's equation. The results in Table 4 (values of β not far from 1) and Fig. 5, indicate that as predicted the Langmuir isotherm best-fits the isotherm data for CR adsorption. So, this model is used, particularly Q_0, for the discussion of the results. The disparity in adsorbate uptakes for different activated carbons may be explained by the textural properties and chemical nature of the prepared samples. The dye removal increased with the increase in both pore volume and surface area. Whereas, the presence of oxygen surface groups on activated carbons disfavours the adsorption of CR dye. It may be observed in Table 4 that the maximum adsorption capacity Q_0 varies in this order C37N < C37 < C37NT. This strongly correlates with basicity of the solid sample from C37N to C37NT (as mentioned above) and with the increase in surface area and pore volume.

Activated carbons are materials with amphoteric character, thus, depending on the pH of the solution. The carbons surface is positively charged at pH < pH$_{pzc}$ favouring the adsorption of anionic species and negatively charged at pH > pH$_{pzc}$, which will favour the adsorption of cationic species [17]. At first sight it could be qualitatively explained only considering electrostatic interactions as the adsorption mechanism, since the anionic dye is negatively charged when dissolved in water. However, the consideration of two parallel mechanisms is necessary to understand and discuss the adsorption of organic solutes on activated carbon, one associated to electrostatic forces and the other to dispersive forces [18]. The latter mechanism arises from the interactions between the delocalized π electrons of the

Table 4
Parameters of the Freundlich Langmuir and Redlich–Peterson models for Congo red adsorption isotherms

Activated Carbon	Freundlich model			Langmuir model			R-P model			
	K_F (mg/g)(mg/l)^n	$1/n$	R^2	Q_0 (mg/g)	K_L (l/mg)	R^2	K_R l/mg	a_R (l/mg)$^{1/\beta}$	β	R^2
C37	5.0	0.43	0.92	83.4	0.009	0.95	0.887	0.015	0.941	0.95
C37N	5.0	0.39	0.96	61.0	0.013	0.99	1.045	0.036	0.876	0.99
C37NT	8.1	0.41	0.94	105.4	0.013	0.96	1.743	0.035	0.876	0.96

Lewis basic sites in the basal planes of activated carbon and the free electrons of the dye molecule present in aromatics rings and multiple bonds. These interactions predominate in basic carbons, since the electron density on the carbon surface is high compared to acid activated carbons.

The oxidized sample (C37N) presents the lowest adsorption capacity. This may be because HNO_3 oxidation produces a large number of surface oxygen groups, which increase the constriction at the entrance of the pores, enhance water adsorption and alter the hydrophilicity and polarity of the activated carbon. Water can adsorb preferentially on oxygen containing groups and form clusters, which hinder the dispersion of dye molecules on the adsorption sites. Also, the acidic surface oxygen groups would attract the free π electrons from the basal planes of the adsorbent, decreasing the π electron density. Such an effect would lead to weaker interactions between the π electrons of the dye ring and the π electrons of the basal planes of the activated carbon, thereby reducing CR uptake [19]. Simultaneously there is an increase in repulsive electrostatic interactions between the anion of the dye and the negatively charged surface of sample C37N (pH > pH_{pzc}).

In summary, the adsorption of anionic dyes onto basic activated carbons is favoured, because of the contributions of electrostatic forces (involving the interaction between the negative charges present in the dye molecules dissolved in water and the positively charged centers on the adsorbent surface that mainly result from the protonation of basal plane sites) and dispersive forces [20].

4. Conclusions

The results reported in this study show that:

The highest congo red adsorption capacity is obtained with heat treated sample C37NT (basic carbon). The presence of acid oxygenated groups on the activated carbon surface is detrimental to the adsorption of the anionic dye. Whereas, the elimination of oxygen surface complexes increases the adsorption capacity.

Adsorption of congo red follows pseudo second-order kinetics. The adsorption process is initially mass transfer controlled and later intra-particle diffusion controlled.

Both Langmuir and Redlich–Peterson equations describe well the adsorption data, indicating that homogenous adsorption occurred.

The mechanism adsorption of the anionic dye CR on activated carbons involves electrostatic and dispersive interactions.

References

[1] H. March and F. Rodríguez-Reinoso, Activated carbon, Elsevier, Amsterdam, 2006.
[2] F. Suárez-García, A. Alonso and J. Tascon, Pyrolysis of apple pulp: chemical activation with phosphoric acid, J. Anal. Appl. Pyrolysis, 63 (2002) 283.
[3] N. Bouchemal, M. Belhachemi, Z. Merzougui and F. Addoun, The effect of temperature and impregnation ratio on the active carbon porosity, Desalin. Water Treat., 10 (2009) 115–120.
[4] N.M. Haimour and S. Emeish, Utilization of date stones for production of activated carbon using phosphoric acid, Waste manage., 26 (2006) 651–660.
[5] S.B. Hartono, S. Ismadji, Y. Sudaryanto and W. Irawaty, Utilization of teak sawdust from the timber industry as a precursor of activated carbon for the removal of dyes from synthetic effluents, J. Ind. Eng. Chem., 6 (2005) 864.
[6] M. Belhachemi, Z. Belala, D. Lahcene and F. Addoun, Adsorption of phenol and dye from aqueous solution using chemically modified date pits activated carbons, Desalin. Water Treat., 7 (2009) 182–190.
[7] R.V.R.A. Rios, J. Silvestre-Albero, A. Sepulveda-Escribano and F. Rodriguez-Reinoso, Liquid phase removal of propanethiol by activated carbon: Effect of porosity and functionality, Colloids Surf. A., 300 (2007) 180–190.
[8] J.L. Figueiredo, M.F.R. Pereira, M.M.A. Freitas, J.J.M. Orfao, Modification of the surface chemistry of activated carbons, Carbon, 37 (1999) 1379–1389.
[9] M.S. Shafeeyan, W.M. Ashri Wan Daud, A. Houshmand, A. Shamiri, A review on surface modification of activated carbon for carbon dioxide adsorption, J. Anal. Appl. Pyrolysis, 89 (2010) 143–151.
[10] A. Khaled, A. El Nemr, A. El-Sikaily, O. Abdelwahab. Treatment of artificial textile dye effluent containing Direct Yellow 12 by orange peel carbon, Desalination, 238 (2009) 210–232.
[11] Z. Belala, M. Jeguirim, M. Belhachemi, F. Addoun and G. Trouvé, Biosorption of basic dye from aqueous solutions by Date Stones and Palm-Trees Waste:Kinetic, equilibrium and thermodynamic studies, Desalination, 271 (2011) 80–87.

[12] N. Kamal Amin, Removal of reactive dye from aqueous solutions by adsorption onto activated carbons prepared from sugarcane bagasse pith, Desalination, 223 (2008) 152–161.

[13] I.D. Mall, V.C. Srivastava, N.K. Agarwal and I.M. Mishra, Adsorption removal of malachite green dye from aqueous solution by bagasse fly ash and activated carbon- kinetic study and equilibrium isotherm analyses, Colloids Surf. A, 264 (2004) 17–28.

[14] B. Boulinguiez, P. Le Cloirec and D. Wolbert, Revisiting the determination of Langmuir parameters application to Tetrahydrothiophene adsorption onto activated Carbon, Langmuir, 24 (2008) 6420–6424.

[15] Y.S. Ho, Selection of optimum sorption isotherm, Carbon, 42 (2004) 2115–2116.

[16] K. Fytianos, E. Voudrias and E. Kokkalis, Sorption–desorption behaviour of 2,4-dichlorophenol by marine sediments, Chemosphere, 40 (2000) 3–6.

[17] F. Rodriguez-Reinoso, The role of carbon materials in heterogeneous catalysis, Carbon, 36 (1998) 159–75.

[18] C. Moreno-Castilla, Adsorption of organic molecules from aqueous solutions on carbon materials, Carbon, 42 (2004) 83–94.

[19] S. Wang, Z.H. Zhu, A. Coomes, F. Haghseresht and G.Q. Lu, The physical and surface characteristics of activated carbons and the adsorption of methylene blue from wastewater, Colloid Interface Sci., 284 (2005) 440–446.

[20] Y. Leon, C.A. Leon, J.M. Solar, V. Calemma, L.R. Radovic, Evidence for protonation of basal plane sites on carbon, Carbon, 30 (1992) 797–811.